Mapping Cancer Markers

November 2015 Update

Summary

A third phase of lung cancer analysis started in the September. The analysis is focused on signatures built from a subset of biomarkers, prioritized similarly to the previous phase, but with additional criteria to eliminate redundancy. Analysis of Phase 2 and early Phase 3 data implies some interesting connections when using protein-protein interaction and biological pathway databases. Once Phase 3 is complete, MCM will switch to an ovarian cancer analysis. We look forward to completing the lung cancer dataset and starting computation on ovarian cancer. With the help of World Community Grid members, we are making new discoveries.

Third phase of lung cancer analysis underway

In the last update, we announced a second, targeted phase of lung cancer signature discovery. We have since moved to a new, third phase in lung cancer analysis: targeting high-scoring, uncorrelated biomarkers. Phase 1 surveyed possible lung cancer signatures drawn from the complete set of biomarkers in our lung cancer dataset. The statistics gathered in this first phase were used to narrow the list of biomarkers to explore in subsequent phases. Phases 2 and 3 explore lung cancer signatures drawn from small sets of high-performing signatures, chosen by two different methods. In Phase 2, we have focused on a 1% subset of biomarkers, selected by the frequency with which each appeared in Phase 1 high-scoring signatures. In Phase 3, we selected a different subset of biomarkers that are both high-scoring and largely uncorrelated to one another.

Correlation is a measure of information shared between two data sources. Two biomarkers are correlated if they exhibit similar patterns in the cancer dataset. For example, two correlated genes might show high activity in one set of tumour samples, low activity in a second set, and average activity in a third. Including two highly-correlated biomarkers in the same signature can reduce the quality of the signature, because they would be contributing redundant information to the signature. For a fixed-size signature, a redundant biomarker would potentially displace another with different information content.

As an analogy, consider the information contained in a small library of textbooks. Say there are three books, *A*, *B*, and *C*. If *A* and *B* are two copies of the same textbook, one of them is redundant. Removing *B* from the library would not change the information contained in the library, and replacing *B* with a different textbook (*D*), would increase the information in the library. If *A* and *B* were similar, but not identical books (e.g., two books on introduction to molecular biology written by different authors), there would still be some overlap in the texts, and a possible advantage to replacing *B* with *D*.

Phase 2 vs phase 3 signature performance

Since the target biomarkers in Phase 3 were selected to be minimally inter-correlated, every signature should be free of redundant information. We therefore hypothesized that Phase 3 signatures would perform better on average than those in Phase 2. Figure 1 shows the surprising results: Phase 2 signatures (potentially containing correlated biomarkers) outperformed Phase 3. We are analysing these results further, to determine the main reasons for the performance drop.

Figure 1. Distribution of signature scores for Phase 2 (black) and Phase 3 (blue) signatures. As expected, larger signatures generally outperform smaller. Surprisingly, Phase 2 signatures outperform Phase 3 on average.

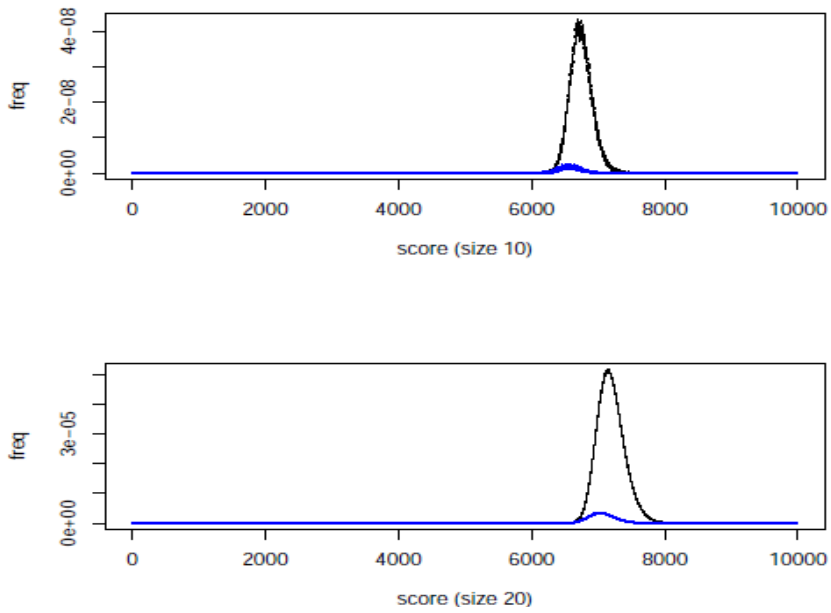

Size effects on biomarker rank in top signatures

Larger signatures (i.e., signatures containing more biomarkers) incorporate more information and can potentially offer better accuracy, but are more complex and expensive to implement in the clinic. MCM has explored lung cancer signatures of multiple sizes for all three phases. For each signature size considered, the target biomarker subsets for Phase 2 were chosen separately, based on Phase 1 statistics. The set of biomarkers selected for Phase 3 is fixed across all signature sizes. This fixed set allows us to compare the effects of signature size on each biomarker's frequency in high-scoring signatures. Figure 2 shows the frequency change when moving from 10 biomarkers per signature to 20. Each dot in the graph represents a biomarker. The X axis represents the frequency with which biomarkers appear in size-10 signatures. The Y axis indicates frequency in size-20 signatures. Note that the biomarkers change in rank but are generally correlated. Size 10 signatures show greater biomarker frequency spread: some have relatively high frequency, and many are low-frequency. The biomarker frequencies in larger (size-20) signatures are more even.

Biomarker pairs as protein interactions?

We applied and extended the analysis of biomarker pairs described in the June 2015 update to early results from Phase 3 data, looking specifically for pairs of biomarkers in both Phase 2 and 3 that appear surprisingly frequently in the highest-scoring lung cancer signatures. When two genes or proteins appear in signatures together with greater frequency than expected randomly, we predict a stronger cancer-related connection (interaction).

We searched for any known connections (interactions) in The Integrated Interactions Database (http://ophid.utoronto.ca/iid/), a database of known and predicted protein-protein interactions created by our lab [1]. We found several interactions in IID that these cancer interactions, but the overlap was not statistically significant.

Figure 2. Biomarker frequencies in size-10 vs. size-20 signatures. Points to the left of the diagonal line represent biomarkers occurring more frequently in size-20 signatures. Note the overall correlation in ranks between sizes, but greater variation in frequencies for shorter signatures.

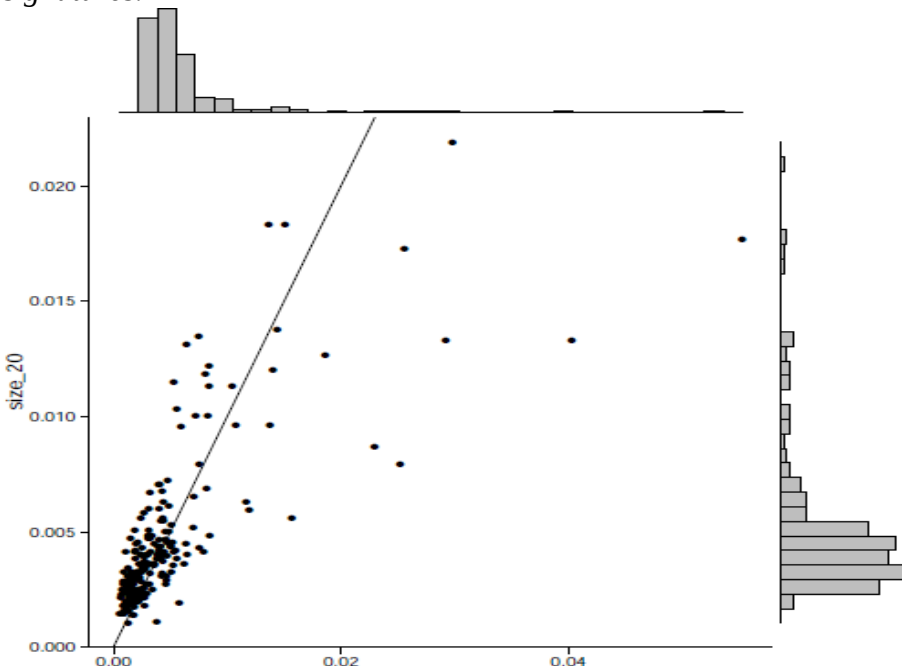

Pathway enrichment in Phase 2 and 3 targets

We also took the genes selected for Phases 2 and 3, and searched for them in a database of biological pathways. See Figure 3. We discovered our lists of genes were enriched (present in statistically significant numbers; $p \leq 0.001$) in several pathways. See Table 1.

Although our analysis is ongoing, we can see that two of the identified pathways are components of

Mevalonate metabolism. Mevalonate pathways are already targets for many drugs such as statins and have been implicated as targets for treatment in lung cancer [2, 3]. Some of the downstream analysis will focus on how the signatures discovered by the World Community Grid processing will ultimately connect to pathways and other research. We have used Mevalonate as an example, but there are many more that can be examined to assess the viability of our best signatures.

Pathway Name	p-value
Mevalonate from acetyl CoA step 2 3	0.003236
Biotinidase Deficiency metabolite pathway	0.004845
Biotin Metabolism	0.004845

Biotinidase Deficiency	0.004845
Multiple carboxylase deficiency neonatal or early onset form	0.004845
Mevalonate biosynthesis	0.004845
Synthesis of Ketone Bodies	0.006449
Ketone Body Metabolism	0.008048
Succinyl CoA 3 ketoacid CoA transferase deficiency	0.008048
Synthesis and Degradation of Ketone Bodies	0.01
Fatty acid triacylglycerol and ketone body metabolism	0.008892
Vitamin H biotin metabolism	0.009643
Dermatan sulfate degradation metazoa	0.009643

Table 1. List of biological pathways enriched with MCM's "discovered-pair" genes. P-values < 0.01 indicate statistical significance.

Figure 3. Biological pathways enriched by biomarker targets in Phase 2 (sizes 10 and 20) and 3 (all sizes). Some pathways are common to all three.

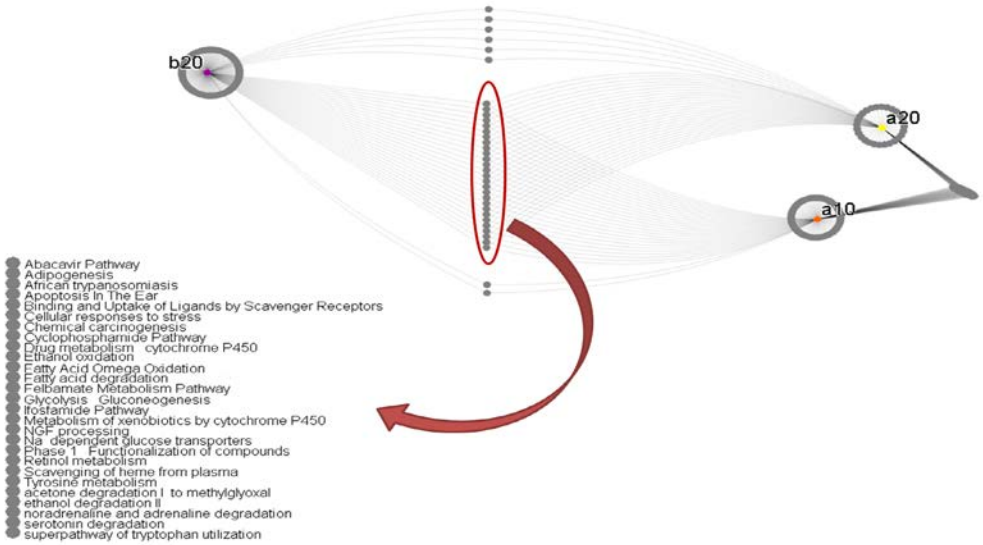

Transition from Lung Cancer to Ovarian Cancer Analysis

Phase 3 is nearly complete, and will be the final piece of MCM lung cancer analysis on World Community Grid before we switch to ovarian cancer.

Ovarian cancer is a gynecologic malignancy that ranks 8th for incidence and 5th for death rate among all women cancers (http://seer.cancer.gov/). The American National Cancer Institute's *Surveillance, Epidemiology, and End Results* (SEER) program estimated 22,240 new cases and 14,030 deaths for ovarian cancer in 2013. Patients are usually diagnosed at an advanced stage (61% present metastasized cancer) and have poor prognosis (27.3 months for metastasized stage (SEER)).

Ovarian cancer was chosen as our next dataset because of long experience with this disease in our own lab, and in those of collaborators (http://www.cs.toronto.edu/~juris/publications.htm). We look forward to using MCM to glean new insights into ovarian cancer.

We expect the transition to ovarian cancer to begin in January, and do not anticipate any interruption in the flow of work units.

Thank you to World Community Grid Members

We wish to thank World Community Grid members for their continued support and interest for this and other projects. Without you, this work would not be possible.

References

1. Kotlyar M, Pastrello C, Sheahan N, Jurisica I. Integrated interactions database: tissue-specific view of the human and model organism interactomes. *Nucleic Acids Res.* 2015 Oct 29
2. Hwa Young Lee, In Kyoung Kim, Hye In Lee, Hye Sun Kang, Chan Kwon Park, Jick Hwan Ha, Seung Joon Kim, Sang Haak Lee. Mevalonate pathway inhibitors as chemopreventive agents on lung cancer cell lines: p53 might be a potent regulator. [abstract]. In: *Proceedings of the Eleventh Annual AACR International Conference on Frontiers in Cancer Prevention Research*; 2012 Oct 16-19; Anaheim, CA. Philadelphia (PA): AACR; Cancer Prev Res 2012;5(11 Suppl):Abstract nr A48.
3. Yano K. Lipid metabolic pathways as lung cancer therapeutic targets: a computational study. *Int J Mol Med*. 2012 Apr;29(4):519-29. doi: 10.3892/ijmm.2011.876. Epub 2011 Dec 30.

Some additional relevant presentations and publications

In several papers we have used strategies described above and protein interaction networks to identify better prognostic markers and new treatment options:

- Singh M, Garg N, Venugopal C, Hallett RM, Tokar T, McFarlane N, Arpin C, Page B, Haftchenary S, Todic A, Rosa DA, Lai P, Gómez-Biagi R, Ali AM, Lewis A, Geletu M, Mahendram S, Bakhshinyan D, Manoranjan B, Vora P, Qazi M, Murty NK, Hassell JA, **Jurisica I**, Gunning P, Singh SK. STAT3 pathway regulates lung-derived brain metastasis initiating cell capacity through miR-21 activation. *Oncotarget* (accepted June 30, 2015, ONC-2014-02546)
- Navab R, **Strumpf D**, To C, Pasko E, Kim KS, Park CJ, Hai J, Liu J, Jonkman J, Barczyk M, Bandarchi B, Wang YH, Venkat K, Ibrahimov E, Pham NA, Ng C, Radulovich N, Zhu CQ, Pintilie M, Wang D, Lu A, **Jurisica I**, Walker GC, Gullberg D, Tsao MS. Integrin a11b1 regulates cancer stromal stiffness and promotes tumorigenecity in non-small cell lung cancer, *Oncogene*, 2015. In press.
- Agostini M, Zangrando A, **Pastrello C**, D'Angelo E, Romano G, Giovannoni R, Giordan M, Maretto I, Bedin C, Zanon C, Digito M, Esposito G, Mescoli C, Lavitrano M, Rizzolio F, **Jurisica I**, Giordano A, Pucciarelli S, Nitti D. A functional biological network centered on XRCC3: a new possible marker of chemoradiotherapy resistance in rectal cancer patients, *Cancer Biol Ther*, **16**(8):1160-71, 2015.
- Agostini M, Janssen KP, Kim LJ, D'Angelo E, Pizzini S, Zangrando A, Zanon C, **Pastrello C**, Maretto I, Digito M, Bedin C, **Jurisica I**, Rizzolio F, Giordano A, Bortoluzzi S, Nitti D, Pucciarelli S. An integrative approach for the identification of prognostic and predictive biomarkers in rectal cancer. *Oncotarget*. 2015. Sep 2.
- Stewart, E.L., Mascaux, C., Pham, N-A, Sakashita, S., Sykes, J., Kim, L., Yanagawa, N., Allo, G., Ishizawa, K., Wang, D., Zhu, C.Q., Li, M., Ng, C., Liu, N., Pintilie, M., Martin, P., John, T., **Jurisica, I.**, Leighl, N.B., Neel, B.G., Waddell, T.K., Shepherd, F.A., Liu, G., Tsao, M-S.

Clinical Utility of Patient Derived Xenografts to Determine Biomarkers of Prognosis and Map Resistance Pathways in EGFR-Mutant Lung Adenocarcinoma, *J Clin Oncol*, **33**(22):2472-80, 2015.

- Camargo, J. F., Resende, M., Zamel, R., Klement, W., Bhimji, A., Huibner, S., Kumar, D., Humar, A., **Jurisica, I.,** Keshavjee, S., Kaul, R., Husain, S. Potential role of CC chemokine receptor 6 (CCR6) in prediction of late-onset CMV infection following solid organ transplant. *Clinical Transplantation*, 2015. In press. doi: 10.1111/ctr.12531
- Fortney, K., **Griesman, G., Kotlyar, M., Pastrello, C., Angeli**, M., Tsao, M.S., **Jurisica, I.** Prioritizing therapeutics for lung cancer: An integrative meta-analysis of cancer gene signatures and chemogenomic data, *PLoS Comp Biol*, **11**(3): e1004068, 2015.

Integrative analyses also help provide better explanations of experimental results and more accurate models:

- Benleulmi-Chaachoua, A., Chen, L., Sokolina, K., Wong, V., **Jurisica, I.**, Emerit, M.B., Darmon, M., Espin, A., Stagljar, I., Tafelmeyer, P., Zamponi, G.W., Delagrange, P., Maurice, P., Jockers, R. Protein interactome mining defines melatonin MT1 receptors as integral component of presynaptic protein complexes of neurons, *Journal of Pineal Research*, In press

Some of this work was presented at multiple meetings and institutions: including keynotes at *The 14th International Conference on Machine Learning* and *Applications* and *The American Society for Blood and Marrow Transplantation, Corporate Council Meeting;* and invited highlight talks at *Intelligent Systems for Molecular Biology Conference* and *Basel Computational Biology Conference.*

Media coverage include:

- In 10 years, 'crowdsourced computing' has changed the world; now it's tackling Ebola, Genevieve Roberts, Independent, June 10; http://www.independent.co.uk/life-style/health-and-families/features/in-10-years-crowdsourced-computing-has-changed-the-world-now-its-tackling-ebola-10311574.html;
- NewsTalk 1010 interview, June 20.

Also, for the second year in a row, Dr. Jurisica has been included in Thomson Reuters highly cited researcher list (http://highlycited.com); Out of 108 in computer science and 3,125 world-wide in 21 fields of science.